Isothermal stress relaxation in electroplated Cu films. I. Mass transport measurements

Dongwen Gan and Paul S. Ho
Laboratory for Interconnect and Packaging, University of Texas, Austin, Texas 78712

Rui Huang[a)]
Department of Aerospace Engineering and Engineering Mechanics, University of Texas, Austin, Texas 78712

Jihperng Leu, Jose Maiz, and Tracey Scherban
Intel Corporation, Hillsboro, Oregon 97214

(Received 22 September 2004; accepted 21 March 2005; published online 13 May 2005)

Recent studies on Cu interconnects have shown that interface diffusion between Cu and the cap layer dominates mass transport for electromigration. The kinetics of mass transport by interface diffusion strongly depends on the material and processing of the cap layer. In this series of two papers, we report in Part I the interface and grain-boundary mass transport measured from isothermal stress relaxation in electroplated Cu thin films with and without a passivation layer and in Part II a kinetic model developed to analyze the stress relaxation based on the coupling of grain boundary and interface diffusion. We show that a set of isothermal stress relaxation experiments together with appropriate modeling analysis can be used to evaluate the kinetics of interface and grain-boundary diffusion that correlate to electromigration reliability of Cu interconnects. Thermal stresses in electroplated Cu films with and without passivation, subjected to thermal cycling and isothermal annealing at selected temperatures, were measured using a bending-beam technique. Thermal cycling experiments showed the effect of passivation and provided information to select the initial stresses and temperatures for isothermal stress measurements. Isothermal experiments at moderate temperatures showed a significant transient behavior of stress relaxation. Based on the kinetic model developed in Part II, grain boundary and interface diffusivities were deduced. While the deduced grain boundary diffusivity reasonably agrees with other studies, the diffusivity at the Cu/SiN cap layer interface was found to be generally lower than the grain-boundary diffusivity at the temperature range of the present study. © *2005 American Institute of Physics*.
[DOI: 10.1063/1.1904720]

I. INTRODUCTION

The formation of Cu damascene interconnect structures require complex processes and structural elements, including electroplating Cu, barrier/seed layers, chemical-mechanical polishing (CMP), and passivation. Recent studies showed that these processes and elements give rise to distinct defect characteristics and mass transport paths, leading to failure mechanisms of electromigration (EM) and stress voiding for Cu interconnects different from Al interconnects.[1–3] Electromigration studies in Cu line structures showed that mass transport is dominated by diffusion at the cap layer interface, probably due to the presence of defects induced by CMP.[4,5] This raised the possibility of reducing interfacial mass transport to improve EM lifetime by optimization of the chemical bonds at the Cu/cap layer interface. Recently, Lane *et al.*[6] showed that the EM lifetime of Cu interconnects can indeed be improved by optimizing the interfacial bond using different cap layers and cleaning processes, and their results were supported by a correlation between the EM lifetime and interfacial adhesion. This was corroborated by Hu *et al.*,[7] who demonstrated a significant improvement in EM lifetime by coating the Cu surface with a thin (20–30 nm) metal layer.

As interconnect scaling advances beyond the 90-nm node, the interface-to-volume ratio continues to increase with decreasing linewidth, making interfacial diffusion increasingly important in contributing to mass transport and thus in controlling the EM reliability of Cu interconnects. EM failure is a complex phenomenon that requires local divergence of diffusion flux. While diffusion processes along interfaces, grain boundaries, and other paths contribute to the overall mass transport, the flux divergent sites are usually associated with localized defects. Therefore, it is difficult to correlate directly the EM lifetime to mass transport and to deduce the diffusivity for the Cu interface. For this reason, we developed a bending-beam method to measure stress relaxation and mass transport in Cu films and line structures. This method has been applied to measure the cap-layer effect on interfacial mass transport in Cu damascene lines, with results found to be consistent with EM and adhesion measurements.[8] In this series of two papers, we report in Part I the experimental results obtained from a stress relaxation study of electroplated Cu films with and without a passivation layer and in Part II a kinetic model developed to analyze stress relaxation by coupling interfacial and grain-boundary

[a)]Electronic mail: ruihuang@mail.utexas.edu

mass transports in thin films. This model was applied to analyze the stress relaxation behavior observed in electroplated Cu films and found to be applicable within certain stress and temperature ranges. The interface and grain boundary diffusivities deduced using this model demonstrate clearly the effect of passivation on interfacial mass transport in electroplated Cu films.

Deformation mechanisms and mass transport processes have been extensively studied for metal films, including e-beam- and sputter-deposited Cu films.[9–14] Several authors have shown that, at moderate temperatures, stress in polycrystalline thin films can be relaxed by diffusion flows at the surface and grain boundary.[10,11,14] Thouless[15] and Gao *et al.*[16] developed diffusional creep models based on coupling of grain boundary and surface diffusion to account for thermal stress behavior under thermal cycling in unpassivated Cu films. Although the stress behavior under thermal cycling is commonly used to investigate mass transport and deformation mechanisms in metal films, it is difficult to delineate diffusion mechanisms when the stress behavior is observed under relatively fast changing temperatures, where steady states are usually not reached. We found stress relaxation observed under isothermal conditions to be more suited for mechanistic studies since the stress variation is observed over a long period of time, where mass transport and deformation can be examined in detail from the initial transient behavior to the steady state. For studies of interconnect metallization, understanding is required for both transient and steady-state stress characteristics, which are important in controlling process yield and long-term reliability.

This paper is organized as follows. We describe first the bending-beam technique and the stress behavior of electroplated Cu films observed under thermal cycling. The experimental conditions were then adjusted to set up proper initial stresses to measure isothermal stress relaxation at selected temperatures. In Sec. III we analyze the experimental results using a kinetic model developed in Part II based on coupling of grain-boundary diffusion with surface and interface diffusion for unpassivated and passivated films, respectively. Section IV applies the model to deduce the grain boundary and interface diffusivities, as well as their temperature dependence from measured stress relaxation data. The details of the kinetic model will be described in Part II of this study.

II. EXPERIMENTAL DETAILS

A. Sample preparation and stress measurement

Cu film samples were prepared on silicon wafers with 200-nm deposited oxides [tetraethylorthosilicate (TEOS)] on both sides. A layer of silicon nitride (SiN) was deposited on one side of the wafer by a chemical vapor deposition (CVD) process, followed by the deposition of a diffusion barrier layer to prevent the Cu atoms from diffusing into the substrate. A Cu seed layer of 100-nm thick was then deposited on the barrier layer by a physical vapor deposition (PVD) process. The rest of the Cu film was prepared by an electroplating process, and the total thickness of the Cu film was 1.0 μm. Some films were further capped with 50-nm SiN and 200-nm silicon oxide as passivation.

Stress in the Cu films was determined using a bending-beam system developed in our laboratory,[17] which determined the thermal stress in the film by measuring the curvature change of the substrate. The stress in a film with a thickness much less than that of the substrate can be calculated using Stoney's equation,

$$\sigma = \frac{E_s h_s^2}{6(1-\nu_s)h}\left(\frac{1}{R}-\frac{1}{R_0}\right), \tag{1}$$

where σ is the film stress, E_s is the Young's modulus of the substrate, h_s is the substrate thickness, h the film thickness, ν_s is the Poisson's ratio of the substrate, R is the radius of the curvature of the substrate with the film, and R_0 is the radius of the curvature of the bare substrate. For the passivated Cu films, since the thickness of the SiN layer is much smaller than that of the Cu film, its contribution to the curvature change was ignored. The contribution from the oxide layer was accounted for using the stress of a bare TEOS film on a Si substrate, as described in Ref. 17. Because R_0 was measured after the film was etched off, the relocation of the sample beams and other uncertainties would induce a system error, estimated to be about 5%.

The samples were cut into 5×40-mm^2 stripes. The surface curvatures were monitored as a function of time and temperature as the samples were thermally loaded in a vacuum chamber under a nitrogen atmosphere at a pressure of 50 torr. In this study, stresses in the Cu films were first measured under thermal cycles, and then isothermal stress relaxation tests were performed at selected temperatures, with various initial stresses based on the thermal cycling stress behavior.

B. Thermal cycling experiments

Figure 1 shows the stress characteristics in a passivated and an unpassivated Cu film during thermal cycling. The ramping rate was set to be 4 °C per minute. During the cooling period, the ramping rate decreased with temperature and could not be held constant for temperatures below 200 °C. During the first cycle (not shown in Fig. 1), the temperature range was from room temperature (RT) to 460 °C, where the films were annealed for 30 min to stabilize their microstructures. During the subsequent cycles, as shown in the figure, the temperature ranges were from RT to 450 °C. Upon initial heating, the stress in both films decreased linearly with temperature, then deviated from the elastic behavior with the onset of plastic deformation. Further increase in temperature resulted in stress changing from tension to compression with increasing plastic deformation. Upon cooling, the compressive stress decreased and then changed to become tensile and reached the initial stress at room temperature, leaving a hysteresis loop as a result of plastic deformation in the film. The shape of the stress curves for the electroplated Cu films in the present study is different from those for e-beam- and sputter-deposited Cu films.[9–11] This indicates an effect of the deposition process on the thermomechanical behavior of Cu films, possibly due to the impurity incorporated during electroplating.

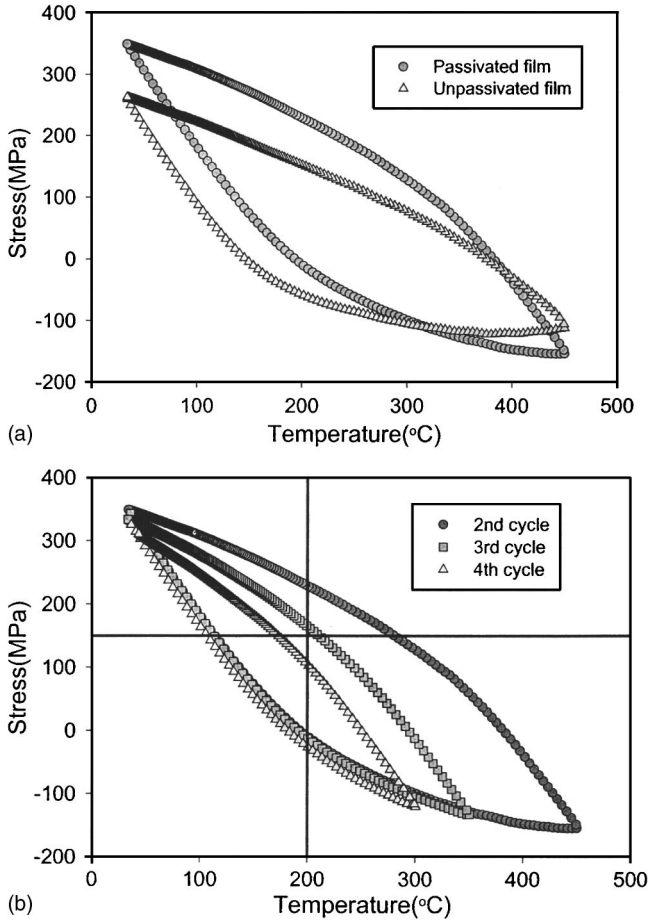

FIG. 1. Thermal stress of the electroplated Cu films in thermal cycles: (a) comparison of the passivated and unpassivated Cu films and (b) stress hysteresis of the passivated Cu film in different thermal cycles.

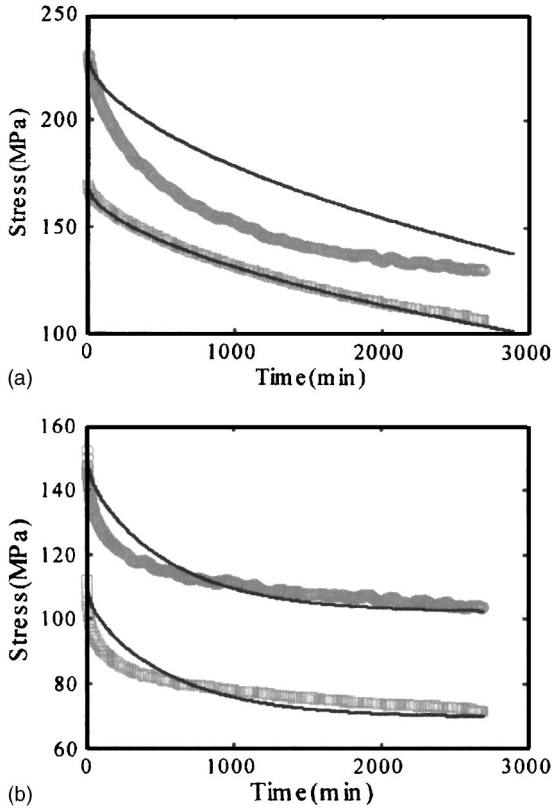

FIG. 2. Stress relaxation of the Cu films at 200 °C from different initial stresses: (a) passivated Cu film and (b) unpassivated Cu film. The solid lines are predicted by the diffusional model.

Comparing to the unpassivated film, the passivated film had a higher residual tensile stress at RT and reached a higher compressive stress at high temperatures. This shows clearly a passivation effect in reducing the amount of inelastic deformation in the film during heating and cooling. This can be attributed to a reduction of the surface mass transport caused by the passivation layer. However, it is difficult to extract quantitative information regarding the change in the surface mass transport rate from the thermal cycling experiments because the continuous change of the temperature and stress may alter the dominant deformation mechanism in Cu films during thermal cycling. Previously, steady-state creep laws have been used to analyze the stress behavior under thermal cycling conditions. However, it will become clear later in analyzing the observed stress relaxation behavior that the steady state is usually not reached during thermal cycling due to a significant transient stage of stress relaxation. In the following, we investigate the kinetics of mass transport by measuring stress relaxation isothermally over a long period, from the initial transient stage to the steady state, and examine the effects of temperature and stress separately.

As shown in Fig. 1(b), by varying the peak temperature, different stress hysteresis can be obtained during thermal cycling, from which one can adjust both the temperature and the initial stress for isothermal measurements. In this way, the effects of stress and temperature can be investigated separately. This is illustrated in Fig. 1(b), where the vertical line indicates that different initial stresses can be obtained at the same temperature to study the stress effect on stress relaxation. Similarly, as sketched by the horizontal line, the same initial stress at different temperatures can be used to study the effect of temperature. This allows us to obtain suitable stress and temperature ranges to study a particular relaxation mechanism. For such studies, the microstructures of the film should remain about the same and not changed after the first cycle. This was supported by the observation using transmission electron microscopy by Dehm *et al.*.[18]

The hysteresis loop of the stress-temperature curves can be roughly divided into four regimes: a low-temperature elastic regime upon heating, an inelastic regime under compression, a high-temperature elastic regime upon cooling, and an inelastic regime under tension. Each of these regimes may be associated with different deformation mechanisms. In particular, we found that the stress relaxation behavior with a compressive initial stress is quite different from that with a tensile initial stress. The stress level and the temperature range for initial tensile stress states seem to be most suited for analysis using the coupled diffusion model, which will be reported in this paper.

C. Isothermal stress relaxation

Figure 2 shows the measured stress relaxation curves of the passivated and unpassivated Cu films for 45 h, starting from different initial stresses at 200 °C. The initial stresses for the passivated film are 230 and 170 MPa, and those for

the unpassivated film are 152 and 112 MPa. The higher initial stress was achieved by cooling the films from 450 °C, and the lower from 350 °C. A higher initial stress resulted in more stress relaxed within a period of 45 h, but still retained a higher stress at the end for both the passivated and unpassivated films. Each curve shows an initial transient behavior, with a sharp decrease of stress with time followed by a steady relaxation. The significance of the transient behavior will become clearer by considering the change in the strain rate as described below.

The total strain in the film consists of an elastic strain and an inelastic strain, and the stress is related to the elastic strain via Hooke's law. Under an isothermal condition, the total strain remains constant, for the film is constrained by the substrate. Over time, the inelastic strain increases and the elastic strain decreases. Consequently, the stress relaxes. The rate of stress relaxation is related to the rate of inelastic deformation as follows:

$$\dot{\sigma} = -M\dot{\varepsilon}_p, \tag{2}$$

where $\dot{\varepsilon}_p$ is the inelastic strain rate, $\dot{\sigma}$ is the measured stress relaxation rate, and M is the biaxial modulus of the film. Accordingly, one can deduce the inelastic strain rate from the stress relaxation curve. The modulus of Cu thin films strongly depends on the film texture due to the mechanical anisotropy of Cu. It may vary from film to film and be different from that of the bulk Cu. The biaxial modulus of the Cu films used in this study was determined from the slope of the elastic regime of the stress-temperature curves obtained from thermal cycling experiments. Using the slopes measured at different temperatures during thermal cycling, the biaxial modulus of the Cu film as a function of temperature was deduced as

$$M = 166.3 - 0.094T + 7.59 \times 10^{-5}T^2, \tag{3}$$

where the biaxial modulus M is in GPa and the temperature T is in °C.

The stress relaxation rate was obtained from the measured relaxation curve using a linear regression fitting. The inelastic strain rate was then calculated using Eq. (2) and plotted in Fig. 3 as a function of stress. A transient behavior of stress relaxation was clearly observed for both passivated and unpassivated films, where the inelastic strain rate was found to depend on the initial stress and the time since the relaxation started. Each curve in Fig. 3 can be roughly divided into an initial transient regime and a steady-state regime, a typical creep behavior. As the starting points of these relaxation measurements were taken from thermal cycling experiments, it confirms that, during thermal cycling, the films had not reached the steady state of inelastic deformation. It is clear that the time to reach the steady state is much longer than that expected from previous studies. Consequently, the transient behavior can significantly affect the thermomechanical behavior under thermal cycling. It is noted that, compared with the passivated Cu film [Fig. 3(a)], the unpassivated Cu film [Fig. 3(b)] took much longer time to reach the steady state and, although the initial stresses were lower, the unpassivated film had higher initial creep rates, which can be qualitatively explained by a kinetic model described in a later section.

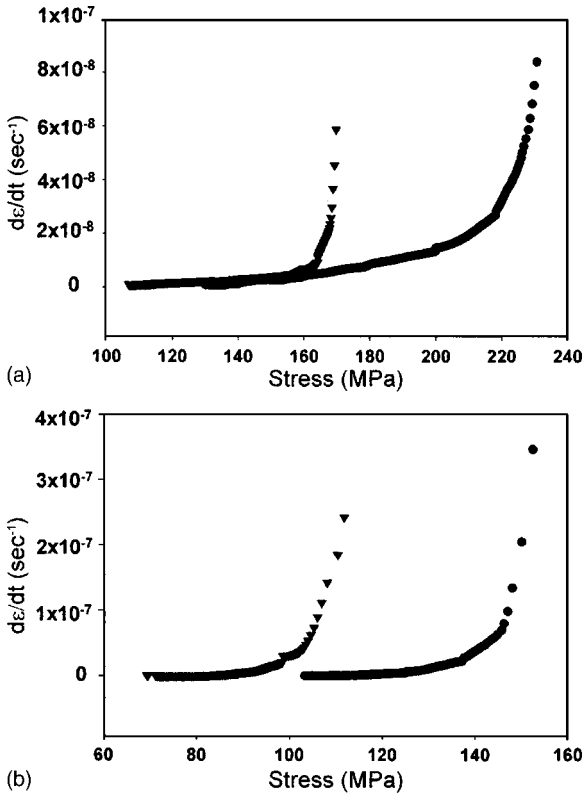

FIG. 3. Creep rate as a function of stress at 200 °C for (a) the passivated Cu film and (b) the unpassivated Cu film.

To study the effect of temperature on stress relaxation, stresses in the passivated Cu film were measured under an isothermal condition at three different temperatures with similar initial stresses, as shown in Fig. 4(a). The unpassivated film was tested at the same temperatures, but with slightly different initial stresses [Fig. 4(b)]. These measurements allow us to extract the temperature dependence of inelastic deformation and, in particular, the activation energy of mass transport. One interesting observation was that, for all the stress relaxation measurements, the stress did not relax to zero within the fairly long period of measurements and in some cases the stresses seem to saturate at some moderate stress levels with no further relaxing. This suggests that there exists a critical stress, below which inelastic deformation does not occur, sometimes called the zero-creep stress.[15,19] However, a simple estimate of the zero-creep stress based on thermodynamics gives a very small stress for the films of present study, much smaller than what appears in the experiments.

III. ANALYSIS OF STRESS RELAXATION

A. Empirical creep analysis

As in bulk materials, creep deformation can be divided into three stages: primary creep, steady-state creep, and ternary creep.[20] The primary creep is often ignored, as the transient stage is short compared to the steady-state stage. For the steady-state creep, the strain rate of a given material is a

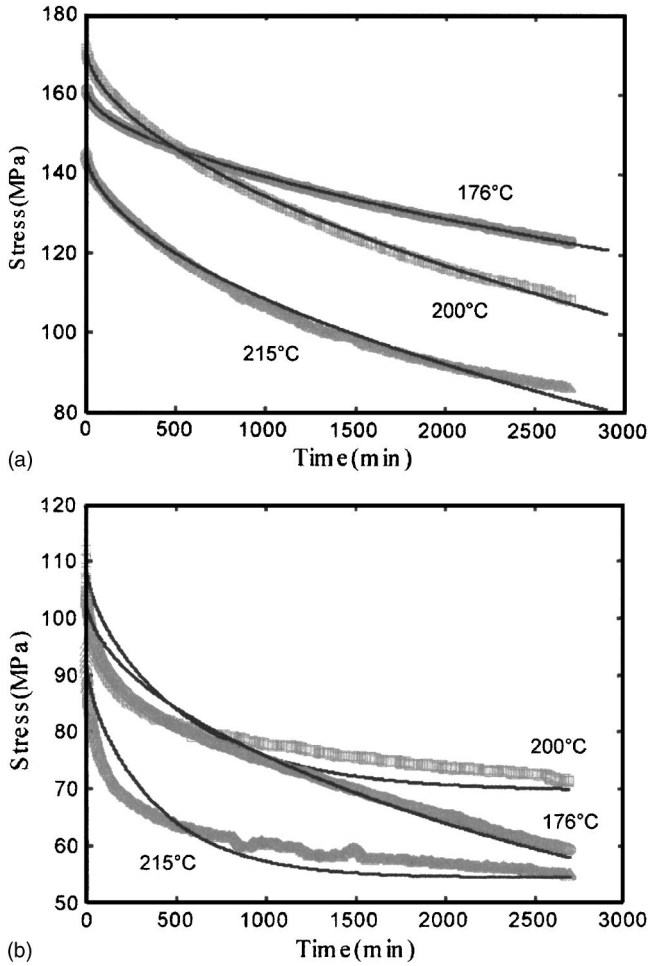

FIG. 4. Isothermal stress relaxation curves at different temperatures of (a) the passivated Cu film and (b) unpassivated Cu film. The solid lines are predicted by the diffusional model.

function of stress and temperature, depending on specific deformation mechanisms such as dislocation gliding and diffusion. The deformation mechanism depends on temperature as well as the stress level, and multiple mechanisms may occur simultaneously. Various steady-state creep laws have been proposed. Of particular interest to the present study is the diffusion mechanism, which usually leads to a linear creep law, such as Coble creep, Nabarro–Herring creep, and their modified forms for thin films.[21] The strain rate by linear creep is

$$\dot{\varepsilon}_p = \frac{\sigma}{\eta}, \tag{4}$$

where η is the creep viscosity, which is a function of temperature but independent of stress. For polycrystalline thin films, the steady-state viscosity can be related to the microstructure and the dominant diffusion paths.[21]

Under the isothermal condition, the total strain of the film is a constant, and the stress relaxes as a result of inelastic deformation, as dictated by Eq. (2). By inserting Eq. (4) into Eq. (2) and integrating over time, one obtains the stress as a function of time

$$\sigma(t) = \sigma_0 \exp(-t/\tau), \tag{5}$$

where $\tau = \eta/M$ is a time constant of stress relaxation and σ_0 is the initial stress.

Equation (5) predicts nearly full relaxation within a period in the order of the time constant τ, while the experiments show much slower relaxation approaching a zero-creep stress state. To account for the transient stage and the zero-creep stress, the following empirical relation was used to describe the stress relaxation,

$$\sigma(t) = \Delta\sigma_1 \exp(-t/\tau_1) + \Delta\sigma_2 \exp(-t/\tau_2) + \sigma_\infty. \tag{6}$$

Here the two exponential terms with different time constants represent the transient stage and the steady state, respectively, and a constant σ_∞ represents the zero-creep stress. With careful choice of the parameters, the stress relaxation behavior observed at different temperatures can indeed be fitted to Eq. (6). However, the parameters obtained by such data fitting do not provide a consistent account for the effects of temperature and initial stress and cannot be used to deduce the diffusivities controlling the relaxation process. In the following section, we will show that the kinetic model developed in Part II, based on the coupling of grain boundary and interface diffusion, includes the relaxation behavior of Eq. (6) as a special case and can be used to deduce the diffusivities.

B. A kinetic model for stress relaxation

In Part II of this study, we describe in detail a diffusion model developed for isothermal stress relaxation based on the coupling of grain-boundary diffusion and interface diffusion, for both passivated and unpassivated polycrystalline films. Similar models have also been developed by Thouless,[15] Gao *et al.*,[16] and Zhang and Gao,[22] all for unpassivated films only. As Cu films in interconnect structures are always passivated, the interface diffusion between the passivated Cu film and the cap layer is of particular interest for electromigration studies. Here we briefly outline the model first and then focus on comparisons between the model and the experiments.

Figure 5 schematically illustrates the model structures for unpassivated and passivated films. For unpassivated films [Fig. 5(a)], we consider mass transport by diffusion along the free surface and the grain boundaries, but neglect lattice diffusion and diffusion along the film/substrate interface. The chemical potential is defined by the local curvature for the surface and the normal stress for the grain boundaries. The gradient of chemical potential drives atoms to diffuse into or out of grain boundaries, relaxing the average stress in the film. The kinetics depends on both the grain-boundary diffusivity and the surface diffusivity, in general. In practice, surface diffusion is often considered faster than grain-boundary diffusion. In this case, it has been shown in Part II that the kinetics is controlled by grain-boundary diffusion, and an approximation can be made by assuming infinitely fast surface diffusion, for which a closed form solution was obtained for stress relaxation of an unpassivated film,

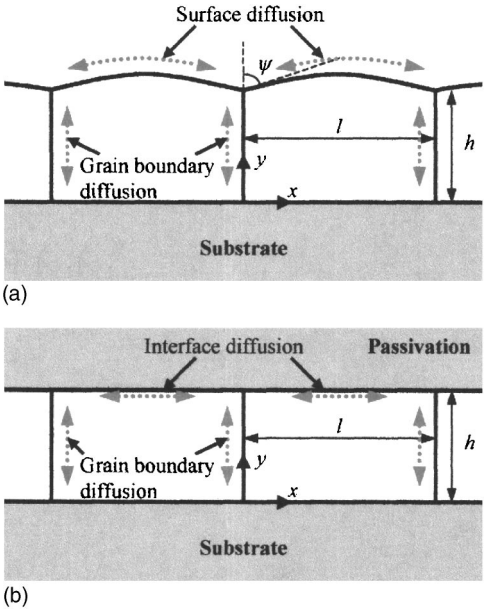

FIG. 5. Schematics of polycrystalline thin films: (a) an unpassivated film and (b) a passivated film.

$$\sigma(t) = \sigma_\infty + (\sigma_0 - \sigma_\infty)\frac{8}{\pi^2}\sum_{n=0}^{\infty}\frac{\exp(-t/\tau_n)}{(2n+1)^2}, \tag{7}$$

where $\tau_n = [4kTh^2 l/(2n+1)^2\pi^2 M\Omega\delta_B D_{B0}]\exp(Q_B/kT)$ and the parameters are film thickness h, grain size l, biaxial modulus M, atomic volume Ω, grain boundary width δ_B, pre-exponential factor for grain-boundary diffusivity D_{B0}, activation energy for grain-boundary diffusion Q_B, and temperature T. In addition, σ_0 is the initial stress and σ_∞ is the zero-creep stress. The zero-creep stress by this model is a result of surface tension and the local equilibrium at the junction of the surface and a grain boundary, i.e.,

$$\sigma_\infty = -\frac{2\gamma}{h}\cos\psi + \frac{\gamma}{h}\sin\psi, \tag{8}$$

where γ is the surface energy density and ψ is the dihedral angle at the junction.

Equation (7) consists of infinite exponential terms, each decaying at a different time scale. Similar solution was obtained by Gao *et al.*[16] The empirical Eq. (6) can be considered to be a special case of this solution, including only two exponential terms. This form of solution exhibits a transient behavior of stress relaxation, in that the stress relaxes faster initially as the high-order terms decay exponentially at high rates and then slows down, with only the first term remaining effective. Figure 6 shows the inelastic strain rate, calculated by inserting Eq. (7) into Eq. (2), as a function of the stress for the unpassivated film relaxing from two different initial stresses at 200 °C. Table I lists the parameters used for this calculation. Comparing to Fig. 3(b), the agreement between the model and the experiments is reasonably good. In particular, the transient behavior is clearly shown by the different strain rates at the same stress and the same temperature from the two different initial stresses.

For passivated films, we consider grain-boundary diffusion coupled with interface diffusion between the Cu film and the cap layer [Fig. 5(b)]. Different from the free surface for unpassivated films, the interface is assumed to remain flat due to the constraint of the cap layer. Mass transport along the interface induces nonuniform local normal stresses, which define the chemical potential and drive interface diffusion. By coupling the interface diffusion with the grain-boundary diffusion, we have shown in Part II that the kinetics of interface diffusion significantly affects stress relaxation behavior in passivated films, especially for the cases when the interface diffusion is slower than grain-boundary diffusion, as commonly assumed for passivated Cu films. In the limiting case when the grain boundary diffusion is infinitely fast, a closed form solution was obtained, taking the same form as Eq. (7) but with a different time scale,

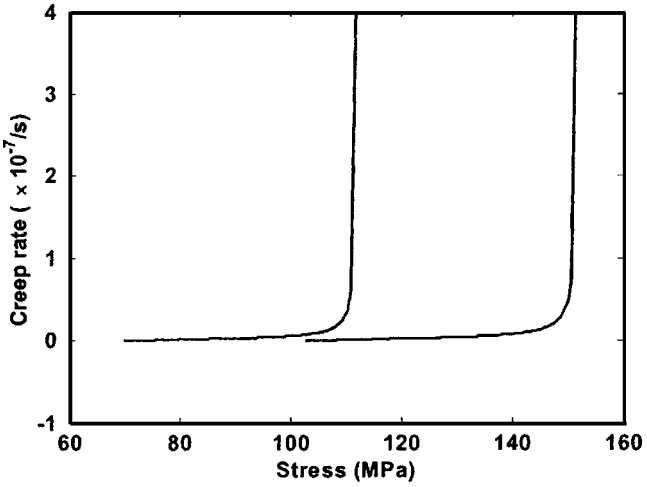

FIG. 6. The creep rate as a function of stress for an unpassivated Cu film at 200 °C predicted by the kinetic model.

$$\tau_n = \frac{kThl^2}{(2n+1)^2\pi^2 M\Omega\delta_I D_{I0}}\exp\left(\frac{Q_I}{kT}\right), \tag{9}$$

where δ_I is the interface width, D_{I0} is the pre-exponential factor for interface diffusivity, and Q_I is the activation energy for interface diffusion.

The stress relaxation curves predicted by the model are plotted in Fig. 2, in comparison with the experimental data for the unpassivated and passivated films. For the unpassivated film [Fig. 2(b)], the closed form solution Eq. (7) is used. However, the zero-creep stress predicted by Eq. (8) is much lower than those extracted from experiments. Without a better understanding of the zero-creep stress, we use the extracted values obtained by the empirical three-term fitting with Eq. (6) for the zero-creep stress and the values in Table I for the other parameters of the Cu film. The agreement

TABLE I. Structure and material parameters for the electroplated Cu films.

Film thickness	$h=1\ \mu$m
Average grain size	$l=1.3\ \mu$m
Pre-exponential grain-boundary diffusivity	$\delta_B D_{B0}=1.1\times10^{-14}$ m^3/s
Activation energy for grain-boundary diffusion	$Q_B=1.07$ eV
Atomic volume	$\Omega=1.18\times10^{-29}$ m^3
Boltzmann's constant	$k=8.617\times10^{-5}$ eV/K

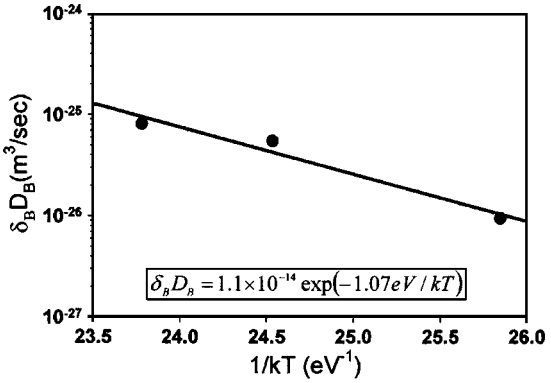

FIG. 7. Deduced grain-boundary diffusivity as a function of temperature from the stress relaxation curves of the unpassivated Cu film.

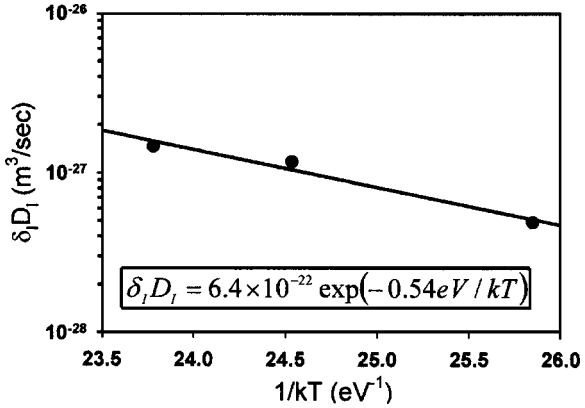

FIG. 8. Deduced interface diffusivity from the stress relaxation curves of the passivated Cu film using the deduced grain boundary diffusivity in Fig. 7.

between the model and the experiments is reasonably good. For the passivated Cu film [Fig. 2(a)], the stress relaxation curves were obtained numerically by assuming that the interface diffusivity is about 5% of the grain-boundary diffusivity and no zero-creep stress was assumed. It is noted that, while the agreement between the model and the experiments is excellent for the case with the lower initial stress (σ_0 =170 MPa), the agreement is poor for the case with the higher initial stress (σ_0=230 MPa). This suggests the existence of different deformation mechanisms at a high stress level, and the diffusion mechanism considered in this model should only be effective within a certain range of temperature and stress levels. With a high initial stress level, for example, the dislocation plasticity may be activated, especially at the initial stage.

IV. GRAIN BOUNDARY AND INTERFACE DIFFUSIVITIES

The isothermal stress relaxation experiments and the diffusion model together allow for the extraction of grain boundary and interface diffusivities. The activation energies can be deduced from the temperature dependence of the diffusivities within the proper range. Then, the diffusivities at other temperatures can be obtained by extrapolation for electromigration studies. The procedure is illustrated as follows.

First, the grain-boundary diffusivity at various temperatures can be obtained by fitting Eq. (7) to the stress relaxation curves of unpassivated films. With other parameters fixed, the grain-boundary diffusivity, $\delta_B D_B = \delta_B D_{B0} \times \exp(-Q_B/kT)$, is varied to minimize the fitting error by means of a least-square optimization. Figure 4(b) shows the stress relaxation curves at 176, 200, and 215 °C and the fitting results. The grain boundary diffusivity $\delta_B D_B$ of the Cu film at 176, 200, and 215 °C were deduced to be 9.5×10^{-27}, 5.5×10^{-26}, and 8.1×10^{-26} m^3/s, respectively. The diffusivities were then fitted into an Arrhenius plot, as shown in Fig. 7, from which we obtain the activation energy and the pre-exponential factor for grain-boundary diffusion: Q_B =1.07 eV and $\delta_B D_{B0}=1.1\times10^{-14}$ m^3/s, which are listed in Table I.

Next, the interface diffusivities at various temperatures are deduced similarly from the stress relaxation curves for passivated Cu films, using the grain-boundary diffusivity deduced above and varying the ratio between the interface diffusivity and the grain-boundary diffusivity for the least-square fitting, as shown in Fig. 4(a). A finite difference method was used to obtain numerical solutions for the coupled diffusion problem; the detail is described in Part II. Alternatively, one may use the closed form solution, Eq. (7), with the time constant in Eq. (9) for the limiting case with relatively fast grain-boundary diffusion to extract the interface diffusivity directly, without knowing the grain-boundary diffusivity. Figure 8 shows the deduced interface diffusivity as a function of temperature, from which we obtain the activation energy and the pre-exponential factor for the interface diffusion: Q_I=0.54 eV and $\delta_I D_{I0}=6.4\times10^{-22}$ m^3/s.

Some previous studies of Cu films have assumed the same grain-boundary diffusivity as in bulk Cu, for which the activation energy is 1.08 eV.[20] Other studies have reported grain-boundary diffusivities measured directly in Cu polycrystals. For example, Gupta *et al.*[23] reported that Q_B =0.95 eV and $\delta_B D_{B0}=2.9\times10^{-15}$ m^3/s. Comparing to these results, the grain-boundary diffusivity extracted in the present study seems to be reasonable. For the interface diffusivity, we are not aware of any previous report. In this study, the extracted interface diffusivity also depends on the grain-boundary diffusivity, due to the coupling of the two diffusion processes. Using the grain-boundary diffusivity by Gupta *et al.*,[23] we obtain that Q_I=0.66 eV and $\delta_I D_{I0}=1.0\times10^{-20}$ m^3/s. In Fig. 9, we compare the two sets of interface diffusivities as well as the grain-boundary diffusivities of the Cu film with the published results by Frost and Ashby,[20] Gupta *et al.*,[23] and Surholt and Herzig.[24] In the temperature range of this study, the interface diffusivity in the Cu film is about two orders of magnitude smaller than the grain-boundary diffusivity, which qualitatively explains the higher strain rates in the unpassivated films [Fig. 3(b)] in comparison with those in the passivated films [Fig. 3(a)].

In submicron Cu lines with a bamboo-like microstructure, the Cu/cap layer interface is believed to be the dominant diffusion path for electromigration and the activation energy determined from the EM lifetime was found to be between 0.8 and 1.2 eV.[4] Obviously, the activation energy, 0.54 or 0.66 eV, deduced in this study is lower than the values measured by the electromigration test. Reasons for this discrepancy may relate to the properties of the interface

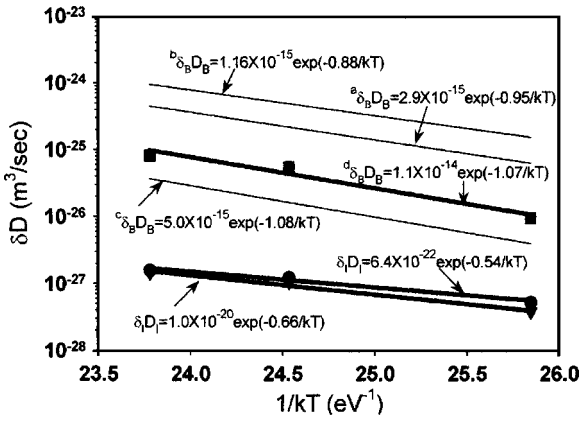

FIG. 9. Comparison of the grain boundary and interface diffusivities with previous studies [[a] Gupta *et al.* (Ref. 23), [b] Surholt and Herzig (Ref. 24), [c] Frost and Ashby (Ref. 20), and [d] this study].

in the passivated Cu film used in this study. EM lifetime is controlled by the mechanism of damage formation, a complex process where the diffusivity is only one of the controlling factors. It may not be surprising that the EM activation energy differs from that obtained for interface diffusion.

V. SUMMARY

In this study, thermal stresses in electroplated Cu films with and without passivation, subjected to thermal cycling and isothermal annealing at selected temperatures, were measured using a bending-beam technique. Thermal cycling experiments showed the effect of passivation, resulting in reduced plastic deformation and higher residual stresses in the passivated film. By adjusting the thermal cycling temperature, the initial stress and temperature can be varied for studying stress relaxation in Cu films. In this way, isothermal stress relaxation measurements were performed for both passivated and unpassivated Cu films as a function of initial stress and temperature. Results indicated a transient behavior for stress relaxation in the Cu films, which lasted longer in the unpassivated Cu film.

A diffusional model coupling grain-boundary diffusion and surface or interface diffusion has been developed to deduce grain boundary and interface diffusivities based on the stress relaxation behavior observed in unpassivated and passivated Cu films. This model predicts the transient behavior observed and is able to account for the experimental results in the stress and temperature range of this study. Based on the kinetic model, grain boundary and interface diffusivities were deduced. The grain-boundary diffusivity was found to be $1.1\times10^{-14}\exp(-1.07\ \mathrm{eV}/kT)$, which is in general agreement with previous measurements. The diffusivity at the Cu/SiN cap layer interface was found to be generally lower than the grain-boundary diffusivity at the temperature range of the present study. Results from this study demonstrated isothermal stress relaxation measurement to be an effective method to evaluate the interface mass transportation in Cu metallization.

ACKNOWLEDGMENTS

This work was supported in part by the Advanced Technology Program of Texas Higher Education Coordinating Board and Intel Corporation. The authors would like to thank Jun He of Intel for helpful discussions.

[1] R. Rosenberg, D. C. Edelstein, C. K. Hu, and K. P. Rodbell, Annu. Rev. Mater. Sci. **30**, 229 (2000).
[2] C. K. Hu and J. M. E. Harper, Mater. Chem. Phys. **52**, 5 (1998).
[3] E. Ogawa, K. D. Lee, and P. S. Ho, IEEE Trans. Reliab. **3**, 403 (2002).
[4] C. K. Hu, R. Rosenberg, and K. Y. Lee, Appl. Phys. Lett. **74**, 2945 (1999).
[5] P. Besser, A. Marathe, L. Zhao, M. Herrick, C. Capasso, and H. Kawasaki, Tech. Dig. - Int. Electron Devices Meet. **2000**, 119.
[6] M. W. Lane, E. G. Liniger, and J. R. Lloyd, J. Appl. Phys. **93**, 1417 (2003).
[7] C. K. Hu *et al.*, Appl. Phys. Lett. **81**, 1782 (2002).
[8] D. Gan, S. Yoon, P. S. Ho, J. Leu, J. Maiz, and T. Scherban, Proc. Advanced Metallization Conference (Montreal, Canada, 2003) (unpublished).
[9] P. A. Flinn, J. Mater. Res. **6**, 1498 (1991).
[10] M. D. Thouless, J. Gupta, and J. M. E. Harper, J. Mater. Res. **8**, 1845 (1993).
[11] R. P. Vinci, E. M. Zielinski, and J. C. Bravman, Thin Solid Films **262**, 142 (1995).
[12] Y.-L. Shen, S. Suresh, M. Y. He, A. Bagchi, O. Kienzle, M. Ruhle, and A. G. Evans, J. Mater. Res. **13**, 1928 (1998).
[13] R. M. Keller, S. P. Baker, and E. Arzt, Acta Mater. **47**, 415 (1999).
[14] R. M. Keller, S. P. Baker, and E. Arzt, J. Mater. Res. **13**, 1307 (1998).
[15] M. D. Thouless, Acta Metall. Mater. **41**, 1057 (1993).
[16] H. Gao, L. Zhang, W. D. Nix, C. V. Thompson, and E. Arzt, Acta Mater. **47**, 2865 (1999).
[17] I.-S. Yeo, Ph.D. thesis, University of Texas at Austin, 1996.
[18] G. Dehm, D. Weiss, and E. Arzt, Mater. Sci. Eng., A **309–310**, 468 (2001).
[19] D. Josell, T. P. Weihs, and H. Gao, MRS Bull. **27**, 39 (2002).
[20] H. J. Frost and M. F. Ashby, *Deformation-Mechanism Maps: The Plasticity and Creep of Metals and Ceramics* (Pergamon, Oxford, 1982).
[21] H. J. Frost, Mater. Res. Soc. Symp. Proc. **265**, 3 (1992).
[22] L. Zhang and H. Gao, Z. Metallkd. **93**, 417 (2002).
[23] D. Gupta, C. K. Hu, and K. L. Lee, Defect Diffus. Forum **143–147**, 1397 (1997).
[24] T. Surholt and C. Herzig, Acta Mater. **45**, 3817 (1997).